

FRACTIONAL STEP METHODS FOR REACTING SHOCK WAVES

Phillip Colella¹, Andrew Majda², and Victor Roytburd³

ABSTRACT. Fractional step schemes are the obvious candidates for use in numerical modelling reacting gases. Per each time step one should have the ingredients (fractional steps) performing the following tasks: 1) integrating the equations of the inviscid fluid dynamics, 2) advancing the chemistry equations, 3) resolving the dissipation mechanisms. The numerical experiments with the inviscid fractional step schemes based on the use of either the Godunov or second order Godunov methods for the fluid dynamics exhibit the following remarkable behaviour: A) For very fine meshes, the Z-N-D wave is completely resolved; B) For moderately fine meshes (i.e., meshes yielding very high resolution in the nonreactive case), a numerical bifurcating wave pattern emerges. The latter pattern is similar to a precursor weak detonation. The explanation of this phenomenon is given within the context of simplified model equations.

1. **INTRODUCTION.** In this paper we discuss several peculiar theoretical and practical computational properties regarding the structure and stability of reacting shock waves. The waves which we study are defined by solutions of the compressible Navier-Stokes or compressible Euler equations for a mixture composed of chemically reacting species in a single space dimension.

The compressible Navier-Stokes equations for a reacting gas

1980 Mathematics Subject Classification 65P05, 76L05, 80A32.

¹Supported by D.O.E. contract AC03-76SF00098

²Partially supported by A.R.O. grant #483964-25530

³Partially supported by N.S.F. grant #DMS84-08260

© 1986 American Mathematical Society
0075-8485/86 \$1.00 + \$.25 per page

are rather complex even in a single space variable, and it is not surprising that simpler model equations for the high Mach number regime have been suggested ([4],[5],[7],[9]). These model systems have transparent analogues of many features of reacting gas equations (see [7],[5] for details).

One of the objectives of this paper is to use the predictions of the simplified model system both for theoretical purposes and as a diagnostic for numerical modelling of the more complex equations of reacting gas flow in the shock wave regime. The authors advocate the use of this simpler model equations for numerical code development for shock phenomena in reacting gases in much the same fashion as the Burgers equation has provided both a wide class of simple test problems and the analysis of difference schemes for the Burgers equation has influenced code development for nonreactive compressible gas flow.

A natural method for numerical simulation of reacting shock waves is provided by fractional step schemes which allow for separate treatment of all the basic physical mechanisms on each time step. We use fractional step schemes with three ingredients per time step: 1) the inviscid hydrodynamics is solved by the Godunov or second order Godunov ([3]) methods; 2) the chemistry equation is advanced by explicit solution of the O.D.E. for each fraction given the temperature; 3) the diffusion equation is solved via the Crank-Nicholson or backward Euler methods. Such a class of numerical schemes is one of the obvious candidates for use in modelling reacting gases given the current development of methods for solving the compressible Euler equations.

One of the objectives of our work here is to assess the performance of the fractional step schemes for different mesh sizes.

This paper is organized as follows: In section 2, we begin by listing the equations of compressible reacting gas flow and describing the simplified model equations; then we describe the numerical methods used in the paper. For the calculations in section 3, the shock layers are fully resolved. Our objectives there are to study the structure and dynamic stability of re-

variable, and it is
ns for the high Mach
], [7], [9]). These model
y features of reacting

s to use the predictions
heoretical purposes and
f the more complex
ck wave regime. The
model equations for
omena in reacting gases
uation has provided
and the analysis of
on has influenced code
gas flow.

tion of reacting shock
mes which allow for
cal mechanisms on each
s with three ingredients
amfcs is solved by the
hods; 2) the chemistry
of the O.D.E. for mass
ffusion equation is
d Euler methods. Such
e obvious candidates
the current development
uler equations.
e is to assess the per-
or different mesh sizes.
In section 2, we begin
reacting gas flow and
; then we describe the
the calculations in
olved. Our objectives
mic stability of re-

acting shock layers on such a length scale where diffusive
mechanisms are important.

Resolving detonation waves on viscous length scales is not a
practical option for a large scale reacting gas computation with
many wave interactions such as the problem of transition to de-
tonation. In section 4, we set all diffusion coefficients to be
zero and investigate the problem of computing the spiked Z-N-D
detonations of the inviscid reacting Euler equations on coarser
meshes. It turns out that for moderately fine meshes (i.e.,
meshes yielding very high resolution is the nonreactive case),
the numerical experiments with the inviscid fractional step
schemes with either the Godunov or second order Godunov method
exhibit a nonphysical bifurcating wave pattern with a structure
similiar to a weak detonation wave. It is worth noting that
qualitatively similar nonphysical wave patterns were reported by
other researches (see [8]).

Finally, in section 5, we give a theoretical explanation for
the computational phenomena on coarse meshes discussed in
section 4.

2. PRELIMINARIES.

The Compressible Navier-Stokes Equations for a Reacting Mixture.

We assume a standard simplified form for the reacting mixture
throughout this paper. Thus, there are only two species
present, unburnt gas and burnt gas, and we postulate that the
unburnt gas is converted to burnt gas by a one-step irreversible
chemical reaction. Under the above hypothesis the compressible
Navier-Stokes equations for the reacting mixture ([10]) are the
system of four equations,

$$\begin{aligned} \rho_t + (\rho u)_x &= 0 \\ (\rho u)_t + (\rho u^2 + p)_x &= \mu u_{xx} \\ (\rho E)_t + (\rho u E + up)_x &= \left(\mu \frac{u^2}{2} \right)_x + c_p (\lambda T_x)_x \end{aligned} \quad (2.1)$$

$$(\rho Z)_t + (\rho u Z)_x = -\rho K(T)Z + (DZ_x)_x$$

where ρ is the density, u is the fluid velocity, E is the total specific energy, and Z is the mass fraction of unburnt gas. The total specific energy, E has the form,

$$E = e + q_0 Z + \frac{u^2}{2} \quad (2.2)$$

with e the specific internal energy and q_0 the amount of heat released by the given chemical reaction. For the assumed ideal gas mixture (with the same γ -gas laws), the pressure and temperature are defined respectively by the formulae $p = (\gamma - 1)\rho e$ and $T = p/\rho R \times M$ with R , Boltzmann's gas constant, M the molecular weight, c_p the specific heat, and γ defined by $c_p(\gamma - 1) = R$. The factor $K(T)$ in (2.1) is strongly dependent on temperature and has the form

$$K(T) = K_0 \phi(T) \quad (2.3)$$

with K_0 the reaction rate. The function $\phi(T)$ typically has the Arrhenius form,

$$\phi(T) = T^a e^{-A/T}$$

or for computational purposes, the approximation for large A given by ignition temperature kinetics,

$$\phi(T) = \begin{cases} 1, & T > T_i \\ 0, & T < T_i \end{cases}$$

with T_i the ignition temperature.

The coefficients μ , λ , and D in (2.1) are coefficients of viscosity, heat conduction, and species diffusion respectively. The compressible Euler equations for the reacting mixture are the special case of (2.1) with $\mu = \lambda = D = 0$.

The Simplified Model Equations. The simplified model equations for the shock wave regime derived through asymptotic limits from

$$Z + (DZ_x)_x$$

the fluid velocity, E is the mass fraction of unburnt gas, E has the form,

$$+ \frac{u^2}{2} \quad (2.2)$$

and q_0 the amount of reaction. For the assumed gas laws, the pressure and γ by the formulae $p = (\gamma - 1)\rho e$ in's gas constant, M the heat, and γ defined by (2.1) is strongly dependent

$$\phi(T) \quad (2.3)$$

function $\phi(T)$ typically has

$$e^{-A/T}$$

approximation for large A tics,

$$T \rightarrow T_i$$

$$T < T_i$$

D in (2.1) are coefficients of species diffusion respectively for the reacting mixture $\mu = \lambda = D = 0$.

The simplified model equations through asymptotic limits from

the system in (2.1) (see [9]) have the form

$$u_t + (u^2/2 - q_0 Z)_x = \beta u_{xx} \quad (2.4)$$

$$Z_x = K\phi(u)Z$$

where u is an asymptotic lumped variable with some features of pressure or temperature, Z is the mass fraction of burnt gas, $q_0 > 0$ is the heat release, $\beta > 0$ is a lumped diffusion coefficient, K is the reaction rate, and $\phi(u)$ has a typical form as described below (2.3). The reader should not be confused by the appearance of Z_x on the left hand side of (2.4) rather than Z_t . The coordinate x in (2.4) is not the space coordinate but is determined through the asymptotics as a scaled space-time coordinate representing distance to the reaction zone; the x -differentiation occurs because Z in (2.4) is convected at the much slower fluid velocity rather than the much faster reacting shock speed (see [9] for the details). With these interpretations the equations in (2.4) become a well-posed problem by prescribing initial data $u_0(x)$ for $u(x, t)$ at time $t = 0$ and prescribing the value of $Z(x, t)$ as $x \rightarrow \infty$ (corresponding to finite values ahead of the reaction zone), i.e., $Z_0(t)$ should be specified with the boundary condition

$$Z_0(t) = \lim_{x \rightarrow \infty} Z(x, t) \quad (2.5)$$

In this paper, we always set $Z_0(t) \equiv 1$ for simplicity.

The Numerical Methods. Now we describe the basic fractional step numerical method used in solving the model equation from (2.4). We set $w = (u, Z)$. Given mesh values $w_j^N = (u_j^N, Z_j^N)$, in the first fractional step we determine $u_j^{N+1/2}$ from u_j^N by using a finite difference approximation to the inviscid Burgers equation

$$u_t + (u^2/2)_x = 0.$$

In our computations we use Godunov's method or a second order

Godunov method ([3]) as the finite difference approximation. In the next fractional step, we determine Z_j^{N+1} as the solution of the O.D.E.

$$Z_x = K\phi(u)Z$$

with u given approximately by $u_j^{N+1/2}$. We march from positive values of x to negative values of x and use the boundary conditions $Z_0 \equiv 1$ on the right end of the large interval where the calculations are carried out. Given the values of $u_j^{N+1/2}$, the above O.D.E. is linear in Z and we solve it by the trapezoidal approximations of the integral in the exact solution formula to derive

$$Z_{j-1}^{N+1} = Z_j^{N+1} \exp \left(\frac{-K\Delta x}{2} (\phi(u_{j-1}^{N+1/2}) + \phi(u_j^{N+1/2})) \right) \quad (2.6)$$

with $Z_j^{N+1} \equiv 1$ for j large enough. Finally, in the third sweep of the fractional step method we solve the diffusion equation

$$u_t - \beta u_{xx} = q_0 Z_x \equiv q_0 K\phi(u)Z. \quad (2.7)$$

The linear diffusion equation on the left-hand side of (2.7) is discretized by using either the backward Euler or Crank-Nicholson methods with initial data $u_j^{N+1/2}$. The value of u_j^{N+1} is then determined by solving this inhomogeneous difference equation where the values for $(u_j^{N+1/2}, Z_j^{N+1})$ are used in the approximation of the forcing function on the extreme right hand side of (2.7) at time level $(N+1)\Delta t$. This completes the description of the basic fractional step method for the simplified model equation. Obviously, the only stability condition needed in the method is the C-F-L condition,

$$\frac{\Delta t}{\Delta x} |u^N| < 1$$

required in the first sweep.

The fractional step algorithms, which we use for the reacting compressible Navier-Stokes equations are organized similarly.

ference approximation. In z_j^{N+1} as the solution

We march from positive and use the boundary the large interval where the values of $u_j^{N+1/2}$, we solve it by the trapezoidal rule in the exact solution

$$\frac{1}{2} + \phi(u_j^{N+1/2})) \quad (2.6)$$

inally, in the third sweep the diffusion equation

$$K_0 \phi(u) Z. \quad (2.7)$$

left-hand side of (2.7) is solved by the Crank-Nicholson method. The value of u_j^{N+1} is then determined by the difference equation where

in the approximation of the right-hand side of (2.7) at time step n . The basic model equation. Obviated in the method is the

which we use for the reacting species are organized similarly.

The same three basic fractional steps are implemented to advance the solution to the next time level. We refer the reader to [2] for details.

3. THE STRUCTURE OF REACTING VISCOUS SHOCKS.

Wave Structure for the Simplified Model System. We begin with a brief summary of the structure of the travelling waves for the model system (2.4) (the details can be found in [7]). Consider a preshock constant state $w_R = (u_R, 1)$ in chemical equilibrium so that $\phi(u_R) = 0$. We study travelling wave solutions of (2.4) with the given preshock state w_R and a fixed speed s . We seek special solutions of (2.4) with the form $w = w(\xi)$, where $\xi = (x-st)/\delta$, so that

$$\lim_{\xi \rightarrow \infty} w(\xi) = (u_R, 1), \quad \lim_{\xi \rightarrow -\infty} w(\xi) = (u_L, 0). \quad (3.1)$$

where u_L needs to be determined. With $Z = q_0 Z$ and $K_0 = \beta K$, substitution of the above form of w into (2.4) leads to the autonomous system of 2 nonlinear O.D.E.'s,

$$u' = u^2 - su - Z + C, \quad Z' = K_0 \phi(u) Z, \quad (3.2)$$

where the integration constant C is determined by w_R . The phase portrait for system (3.2) is depicted in Figure 1. The saddle point $(u_L^*, 0)$ and the nodal point $(u_R^*, 0)$ are the only limiting values for the travelling wave solutions when $\xi \rightarrow \pm\infty$. They correspond to the weak and strong detonation waves propagating with speed s and determined by the Chapman-Jouguet theory. Thus, for a fixed positive value of $K_0 = \beta K$, there is a critical heat release, q_{CR} , so that

- For $q_0 > q_{CR}$, a strong detonation travelling wave profile with speed s exists connecting $(u_R, 1)$ to $(u_L^*, 0)$.
- For $q_0 = q_{CR}$, a weak detonation travelling wave with speed s exists connecting $(u_R, 1)$ to $(u_L^*, 0)$.
- For $q_0 < q_{CR}$, no combustion wave moving with speed s is possible.

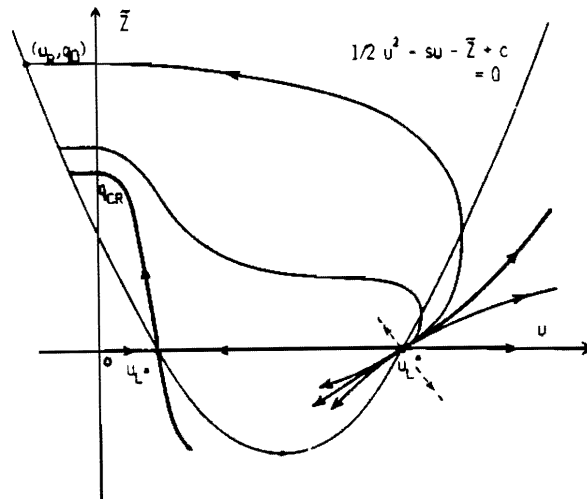


Figure 1.

A similar behavior occurs if the heat release is fixed and K_0 is varied: strong detonations for $K_0 < K_{CR}$, no connecting profiles for $K_0 > K_{CR}$ (see [7]). We make this remark because the reaction rate is the quantity actually varied in some calculations reported below.

Graphs of the typical wave profiles as the heat release is varied, are presented in Figure 2.

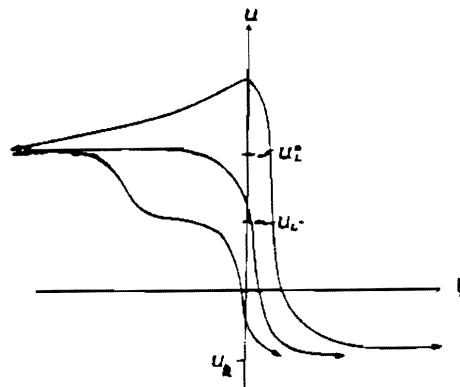


Fig. 2. Shape of travelling wave profiles.



The question of dynamical stability of these profiles was addressed in [2]. In numerical experiments the special initial data,

$$u_0(x) = \begin{cases} u_R, & x > 0 \\ u_L, & x < 0 \end{cases}, \quad Z_0(x) = \begin{cases} q_0, & x > 0 \\ 0, & x < 0 \end{cases} \quad (3.3)$$

with $q_0 > q_{CR}$, evolve to the strong detonation wave moving with speed s . (Note that the data in (3.3) define an inviscid strong detonation of speed s). Thus, numerical calculations of [2] demonstrate the dynamic stability of strong detonation waves in the model.

Of special importance for us is the question, what happens when q_0 is below the critical level, $q_0 < q_{CR}$, so that no traveling wave profile moving at speed s occurs. In this case, the "shock tube" initial data (3.3) evolve into the following bifurcating wave pattern: An approximately self-similar wave pattern given by the weak detonation moving with speed s' , $s' > s$, followed by a fluid dynamics viscous shock moving with the speed $s^* < s$. This wave pattern is illustrated by the graphs in Figure 3. The graph of Z included in the last diagram shows that the

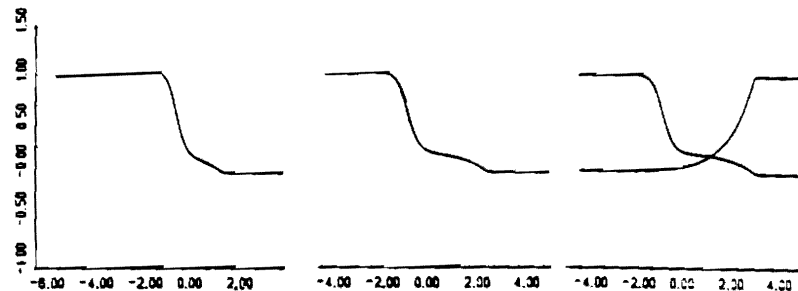


Fig. 3. The bifurcating wave pattern at 160, 320, and 400 time steps.

chemical energy is released in the precursor wave. Note that the graphs are presented in the coordinate system moving with speed s .

e profiles.

Wave Structure for the Reacting Compressible Navier-Stokes Equations. The theory of combustion wave profiles for the reacting gas flow equations from (2.1) is considerably less complete than that for the model equations. Nevertheless, Gardner [6] has recently proved the existence of viscous strong (and weak) detonations for varying (and exceptional) values of the heat release and wave speed. One consequence of the results in [6] is a scenario for the wave structure with varying heat release qualitatively similar to that discussed above for the model equations; in fact, his method of proof involves deformation to the traveling waves of the qualitative model from [7]. This fact both provides a partial rigorous justification for the model and also suggests that similar dynamically stable wave structures, as described earlier in this section for the model, would also occur for the reacting compressible Navier-Stokes equations. The numerical experiments that we discuss in the remainder of this section, confirm this conjectured behavior.

We use the fractional step method with the second order Godunov method for the inviscid hydrodynamics sweep. We introduced the rescale variable $Z = q_0 Z$ rather than Z and the initial data was always taken as the piecewise constant initial data defining a C-J (Chapman-Jouguet) detonation; i.e., the initial data for (p, ρ, u, Z) had the form

$$\begin{aligned} (p_0, \rho_0, 0, q_0) &, \quad x > 0 \\ (p_1, \rho_1, u_1, 0) &, \quad x < 0 \end{aligned}$$

where given the preshock state for $x > 0$, the post-shock state defined for $x < 0$ satisfied the Rankine-Hugoniot relations defining a C-J detonation. The numerical calculations were performed on a finite interval with Dirichlet boundary conditions, and to avoid the computational expense of a very long interval, the solution was allowed to run until the wave came within a fixed number of zones from the right edge of the grid; then the solution was shifted from the right to the left to keep it fixed on the interval. Our graphical displays retain this computa-

ible Navier-Stokes

profiles for the reacting profiles are less complete than for the model. In fact, Gardner [6] has shown that the results of the strong (and weak) detonation waves of the heat release results in [6] is a qualitative agreement with the model equations; the formation of the traveling wave structures, as described by the model, would also occur for the numerical solution of these equations. The numerical results of this section,

with the second order numerical scheme sweep. We introduce the initial data for the constant initial data for the initial condition, i.e., the initial

> 0

< 0

the post-shock state Hugoniot relations defined by the boundary conditions, and to a long interval, the wave came within a fixed distance of the grid; then the wave was left to keep it fixed and retain this computa-

tional artifact and focus on the fastest moving wave pattern.

In this section, diffusive length scales are completely resolved computationally, but for emphasis we will work in dimensional (CGS) units which are typical ones for a viscous reacting shock layer. The detonation waves which we study have fairly small heat release and are modeled on initial data for the pre-shock state corresponding to 25% ozone and 75% oxygen at roughly room temperature in the ozone decomposition C-J detonation.

The first series of calculations is concerned with the emergence of a strong detonation wave from the C-J initial data described above. The pressure and chemical energy profiles of the solution are given in Figure 4. This solution is numerically steady in a reference frame moving with the wave speed.

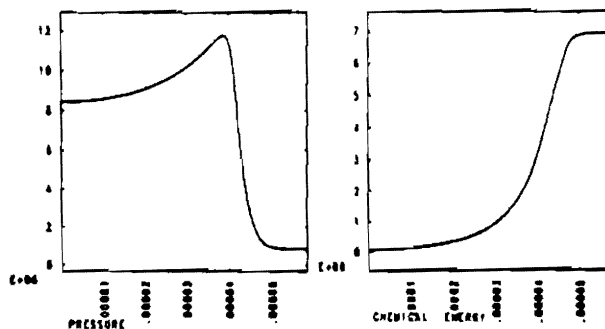


Fig. 4. Dynamically emerging C-J detonation wave.

For the second series of dynamic calculations, we increased (somewhat arbitrarily) the reaction rate fivefold. All other parameters and the initial C-J data were kept fixed. By analogy with the model system, one might anticipate a bifurcation wave pattern if the reaction prefactor K_0 and the heat release q_0 satisfy $q_0 < q_{CR}(K_0)$. The time series of solutions is presented in Figure 5, where only the pressure and chemical energy plots are displayed. As is apparent from the chemical energy plot, all the chemical energy is released in the precursor weak detonation wave as anticipated in the model system. The slower moving trailing wave profile is an ordinary fluid dynamic shock.

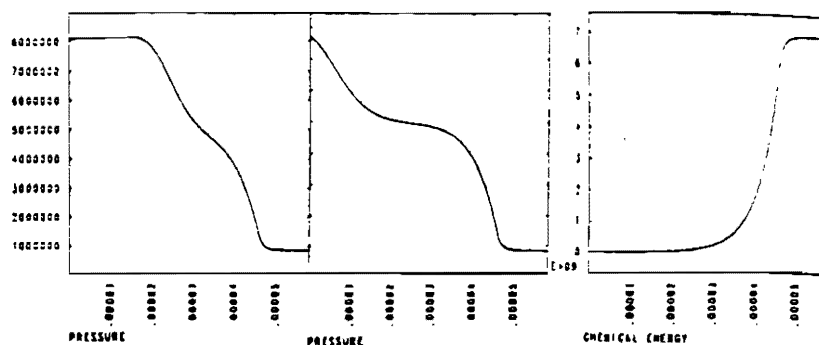


Fig. 5. Dynamically emerging precursor weak detonation at 218 and 424 time steps.

The calculations described above were performed with the space resolutions $\Delta x = 25A$ (Figure 4) and $\Delta x = 15A$ (Figure 5). With these mesh sizes the shocks and the reaction zones are fully resolved (~ 50 meshpoints in the shocks, ~ 200 meshpoints in the reaction zones). We remark that the same wave structures emerged under mesh refinements.

4. INVISCID CALCULATIONS.

The computational meshes used in the calculations from section 3 are several orders of magnitude finer than those that could be used in a typical large scale computing problem. On much larger spatial scales the effects of diffusion are ignored so in this section we report on calculations with the inviscid reacting compressible Euler equations. Since it is an interesting problem to develop numerical methods which can capture the significantly higher pressure peaks which occur in the structure of Z-N-D waves, we assess the performance of the inviscid fractional step methods in such a calculation. We note that any algorithm based on the C-J theory alone (such as [1]) automatically will ignore the Z-N-D pressure spike in the travelling wave structure no matter how fine a mesh is used.

For comparison, we used as initial data the same C-J detona-

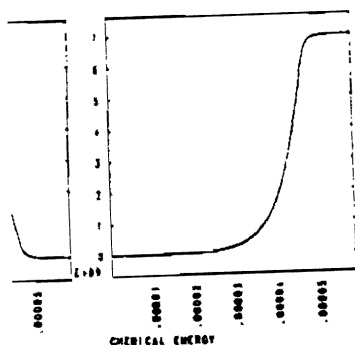


Figure 5. Precursor weak detonation.

are performed with the space $\Delta x = 15A$ (Figure 5). With reaction zones are fully resolved, ~ 200 meshpoints in the same wave structures emerged

the calculations from section 3 are more than those that could be expected. On much larger meshes, the reaction zones are ignored so in this case the inviscid reacting components are an interesting problem to capture the significantly different structure of Z-N-D waves. The fractional step methods and any algorithm based on the Godunov scheme will ignore the wave structure no matter how fine the data. The same C-J detona-

tion wave which we used previously in section 3. In the calculations reported below we always used 300 mesh points while the mesh size and the computational domain were changing. We took $\Delta x = \alpha R_0$ where α is varied from 0.1 to 10^5 . The constant $R_0 = 500A$ is a characteristic length scale which measures the internal structure of the reaction zone whose width is roughly $30 R_0$.

The graphs in Figure 6 display the values of the pressure and chemical energy for the travelling waves that emerged from these

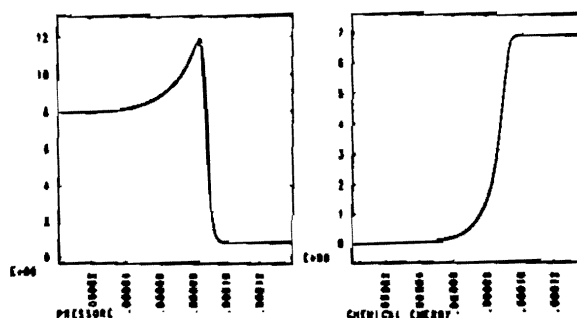


Fig. 6a. $\Delta x = .1 R_0$

calculations with the C-J initial data.

For $\Delta x = .1 R_0$, the reaction zone was completely resolved and the expected Z-N-D profile was computed by either method. Already at $\Delta x = 10 R_0$, neither numerical method has any pressure peak higher than 8 atm. On this mesh the Godunov scheme already clearly exhibits a numerical bifurcating weak detonation pattern qualitatively similar to the one described in section 3 with all chemical energy released too soon in the precursor numerical weak detonation wave. The second order Godunov method also exhibits an incorrect wave pattern on this mesh. On a mesh with $\Delta x = 10^2 R_0$, both methods exhibited totally non-physical bifurcating wave patterns with precursor numerical weak detonations. On even

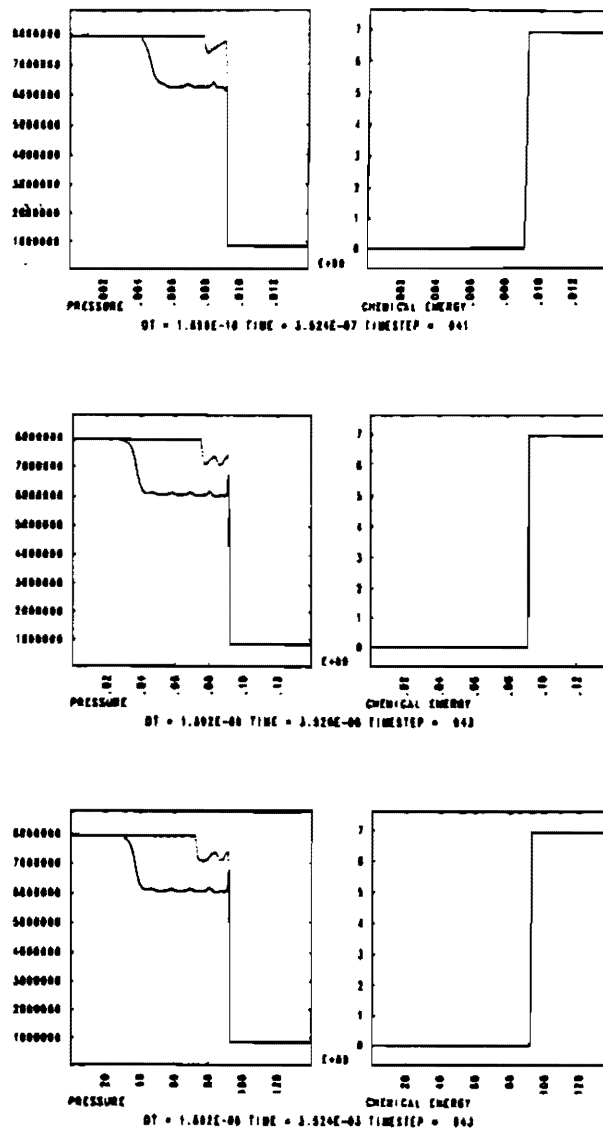
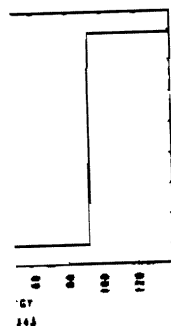
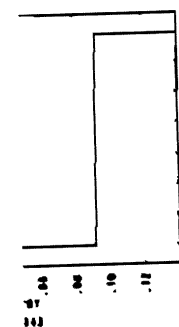
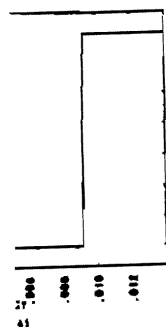


Fig. 6. Dynamically emerging numerical wave patterns with meshes $\Delta x = 10 R_0$, $10^2 R_0$, and $10^5 R_0$. (The black line represents the Godunov method while the dashed line represents the high order Godunov method.)



ve patterns with meshes
k line represents the
sents the high order

coarser meshes, the same approximately self similar non-physical discrete wave pattern emerged as indicated by a comparison of the graphs in Figure 6d with $\Delta x = 10^5 R_0$ and Figure 6c with $\Delta x = 10^2 R_0$. We recall that the mesh with $\Delta x = 10^5 R_0$ has 300 mesh points in a region only 1.5 meters long. Although we do not report the detailed time history here for these calculations, the numerical weak detonation wave that emerges is always moving at the speed of one mesh point per time step.

A similar computational phenomena occurred for the fractional step schemes for the model system with the Godunov or second order Godunov methods.

5. DISCRETE WEAK DETONATIONS.

The calculations from section 4 on coarser meshes with the Godunov fractional step schemes yield a bifurcating numerical pattern with a discrete weak detonation wave as a precursor. These wave patterns qualitatively resemble the analytic bifurcating wave structures documented as stable exact solutions of the reacting Navier-Stokes equations in section 3. However, the wave patterns from section 4 are purely a numerical artifact since the numerical solution converged to the expected Z-N-D detonation under further mesh refinement.

Here we provide a theoretical explanation for the numerical results presented in section 4. We work within the context of the simplified model and derive a class of nonphysical discrete traveling waves for the basic inviscid fractional step scheme introduced in section 2. These exact solutions of the difference equations will be numerical weak detonations moving at the speed, $s' = \Delta x / \Delta t$, i.e., one grid spacing per time step, as observed in the calculations from section 4. The (numerical) stability of such discrete weak detonations has been demonstrated in the calculations reported in section 4 for sufficiently coarse meshes.

We consider the problem of computing the Z-N-D detonation dynamically as a solution of the system

$$\begin{aligned} u_t + (u^2/2 - q_0 Z)_x &= 0 \\ Z_x &= K\phi(u)Z \end{aligned} \quad (5.1)$$

with initial data given by a C-J detonation wave for the fixed wave speed s , i.e., with the initial data having the form (3.3). These initial data should satisfy the reacting Hugoniot equation

$$H(u_L^*, u_R, s) = q_0$$

where $H(u, v, s) \equiv s(u-v) - (u^2 - v^2)/2$ is the Hugoniot function.

We are interested in wave solutions of a difference version of (5.1) travelling with the speed $s' = \Delta x / \Delta t$. First, we note that s' should be larger than s . Indeed, the C-F-L stability condition requires $(\Delta t / \Delta x) u_L^* = \alpha < 1$, i.e., $s' > u_L^*$. On the other hand, $u_L^* > s > u_R$. It yields $s' > s$. Now it is easily seen that since $s' > s$, the quadratic equation

$$H(u, u_R, s') - q_0 = 0$$

has two solutions u_L^* and u_{L*} , and that

$$u_L^* > s' > u_L^* > u_{L*} > u_R.$$

The main result of this section is concerned with the existence of a travelling wave solution $w_j^N = (u_j^N, Z_j^N)$ of the difference scheme approximating (5.1) which has these properties:

A) It travels with speed s' , i.e.,

$$w_j^N = w_{j-1}^{N-1} = \dots = w_{j-k}^0 \quad \text{for all } N > 0 \text{ and } j. \quad (5.2)$$

B) It approximates an inviscid weak detonation wave which connects the states $(u_R, 1)$ and $(u_L^*, 0)$:

$$w_j^0 = (u_R, 1), \quad j > 0; \quad \lim_{j \rightarrow -\infty} w_j^0 = (u_L^*, 0). \quad (5.3)$$

Such solutions of the numerical scheme define the discrete weak detonations moving at mesh speed which were observed computationally in the last section.

$$= 0 \quad (5.1)$$

on wave for the fixed
a having the form (3.3).
ating Hugoniot equation

Hugoniot function.
s of a difference version
x/Δt. First, we note
, the C-F-L stability
e., $s' > u_L^*$. On the
s. Now it is easily
ation

0

u_R .

ncerned with the exis-
(u_j^N, Z_j^N) of the difer-
these properties:

$$> 0 \text{ and } j. \quad (5.2)$$

ation wave which con-

$$= (u_L^*, 0). \quad (5.3)$$

fine the discrete weak
re observed

For simplicity we assume that the initial data (3.4) satisfy $u_R > 0$. In this case the wave speeds are positive and Godunov's scheme reduces to the upwind scheme.

PROPOSITION (Existence of Numerical Weak Detonations). For the inviscid fractional step scheme based on the upwind scheme, explicit nonphysical travelling waves satisfying (5.2) and (5.3) exist under the following conditions on heat release q_0 , reaction rate K , and mesh spacing Δx :

- A) For ignition temperature kinetics with ignition temperature \tilde{u} satisfying $\tilde{u} > u_R$, nonphysical discrete travelling waves with a monotone profile exist provided the two explicit inequalities

$$\tilde{u} < u_{L^*} \text{ and } H(\tilde{u}, u_R, s') < q_0 \left(1 - e^{-\frac{K\Delta x}{2}}\right) \quad (5.4)$$

are satisfied.

- B) For a general kinetics structure function $\phi(u)$ satisfying $\phi(u_R) = 0$ and $\phi(u) > 0$ for $u_R < u$, a numerical weak detonation profile exists provided that there is a solution u_0 with $u_R < u_0 < u_L^*$ to the nonlinear algebraic equation

$$H(u_0, u_R, s') + q_0 e^{-\frac{K\Delta x}{2}\phi(u_0)} = q_0. \quad (5.5)$$

The proposition is proved by the effective construction of the solution of the equation

$$w_j^1 = w_{j-1}^0 \quad (5.6)$$

where w^1 is a nonlinear function of w^0 given by the marching formulas of the difference scheme. Equation (5.6) is solved recursively, $w_j = (u_R, 1)$ for $j > 1$, w_j is generated from w_{j+1} for $j < 0$. The solvability of (5.6) is guaranteed by the conditions (5.4) or (5.5). We refer the reader to [2] for the detailed proof.

In conclusion we note that any of the quantitative algebraic

conditions in (5.4) or (5.5) is satisfied if either

A) $K' \equiv K\Delta x$ is large enough or

B) the heat release q_0 is large enough for a fixed mesh.

In fact K' for these inviscid methods for reacting gas plays an analogous role as the mesh Reynolds number in viscous incompressible flow. The behavior of the numerical method for K' large for the reacting compressible Euler equations mimics the behavior for high reaction rate K_0 documented in section 3 for the reacting compressible Navier-Stokes equations.

The explicit conditions for the existence of numerical weak detonations provide a quantitative guideline for the validity of the basic fractional step schemes in coarser mesh calculations.

BIBLIOGRAPHY

1. Chorin, A., "Random choice methods with applications to reacting gas flow", J. Comp. Phys. 25, 253-272 (1977).
2. Colella, P., A. Majda, and V. Roytburd, "Theoretical and numerical structure for reacting shock waves", to appear in SIAM J. Sci. Stat. Computing.
3. Colella, P., and Woodward, P., "The piecewise-parabolic method (PPM) for gas-dynamical simulations", J. Comp. Phys. 54, 174-201 (1984).
4. Fickett, W., "Detonation in miniature", Amer. J. Phys. 47, 1050-1059 (1979).
5. Fickett, W., Detonation in Miniature, University of California Press, Berkeley, Ca. (1985).
6. Gardner, R., "On the detonation of a combustible gas", Trans. Amer. Math. Society 277, 431-468 (1983).
7. Majda, A., "A qualitative model for dynamic combustion", SIAM J. Appl. Math. 41, 70-93 (1981).
8. Nunziato, J. W., and M.E. Kipp, "Numerical studies of initiation, detonation, and detonation failure in nitromethane", Sandia Report, SAND81-0669 (1983).
9. Rosales, R. and Majda, A., "Weakly nonlinear detonation waves", SIAM J. Appl. Math. 43, 1086-1118 (1983).
10. Williams, F. A., Combustion Theory, Addison-Wesley, Reading, Mass. (1965).